

Trafficking Defects and Gating Abnormalities of a Novel *SCN5A* Mutation Question Gene-Specific Therapy in Long QT Syndrome Type 3

Yanfei Ruan, Marco Denegri, Nian Liu, Tiziana Bachetti, Morena Seregni, Stefano Morotti, Stefano Severi, Carlo Napolitano, Silvia G. Priori

Rationale: Sodium channel blockers are used as gene-specific treatments in long-QT syndrome type 3, which is caused by mutations in the sodium channel gene (*SCN5A*). Response to treatment is influenced by biophysical properties of mutations.

Objective: We sought to investigate the unexpected deleterious effect of mexiletine in a mutation combining gain-of-function and trafficking abnormalities.

Methods and Results: A long-QT syndrome type 3 child experienced paradoxical QT prolongation and worsening of arrhythmias after mexiletine treatment. The *SCN5A* mutation F1473S expressed in HEK293 cells presented a right-ward shift of steady-state inactivation, enlarged window current, and huge sustained sodium current. Unexpectedly, it also reduced the peak sodium current by 80%. Immunostaining showed that mutant Nav1.5 is retained in the cytoplasm. Incubation with 10 $\mu\text{mol/L}$ mexiletine rescued the trafficking defect of F1473S, causing a significant increase in peak current, whereas sustained current was unchanged. Using a Markovian model of the Na channel and a model of human ventricular action potential, we showed that simulated exposure of F1473S to mexiletine paradoxically increased action potential duration, mimicking QT prolongation seen in the index patient on mexiletine treatment.

Conclusions: Sodium channel blockers are largely used to shorten QT intervals in carriers of *SCN5A* mutations. We provided evidence that these agents may facilitate trafficking of mutant proteins, thus exacerbating QT prolongation. These data suggest that caution should be used when recommending this class of drugs to carriers of mutations with undefined electrophysiological properties. (*Circ Res.* 2010;106:1374-1383.)

Key Words: electrophysiology ■ genetics ■ long-QT syndrome ■ pharmacology ■ ion channels

Long-QT syndrome is an inherited arrhythmogenic disease characterized by QT interval prolongation and susceptibility to ventricular tachyarrhythmias. Long-QT syndrome type 3 (LQT3) is a variant of long-QT syndrome characterized by high lethality,¹ marked prolongation of repolarization, poor response to β -blockers,² and cardiac events occurring preferentially at rest. LQT3 is caused by mutations in the *SCN5A* gene that encode for the α subunit of the channel that conducts the inward sodium current responsible for fast depolarization and critical for maintenance of intracardiac conduction.^{3,4} Following the identification of the first *SCN5A* mutation published in 1995,⁵ more than 80 *SCN5A* mutations have been identified in LQT3 patients.

SCN5A mutations associated with LQT3 increase the sodium current by augmenting either the sustained sodium

current (I_{sus}) or the window current, thus prolonging cardiac repolarization.⁶ Based on this evidence, the use of sodium channel blockers to treat LQT3 patients and reduce QT interval has been proposed. Early in vitro studies⁷ demonstrated that mexiletine is effective in shortening action potential duration (APD) in cardiac myocytes exposed to anthopleurin, a compound that mimics LQT3 cellular phenotype. Furthermore early clinical studies on the use of mexiletine or flecainide were successful in shortening repolarization^{8,9} and paved the way to the clinical use of sodium channel blockers in LQT3 patients as a gene-specific therapy.

As the experience with the use of these drugs accumulated, the early enthusiasm was dimmed, and it became clear that flecainide might not be always appropriate for LQT3 patients. Indeed, the response of selected mutations could induce an

Original received September 12, 2009; resubmission received February 12, 2010; revised resubmission received March 10, 2010; accepted March 11, 2010.

From the Cardiovascular Genetic Program (Y.R., N.L., C.N., S.G.P.), Leon H. Charney Division of Cardiology, New York University School of Medicine; Molecular Cardiology (M.D., T.B., M.S., C.N., S.G.P.), IRCCS Fondazione Salvatore Maugeri, Pavia, Italy; and Biomedical Engineering Laboratory (S.M., S.S.), DEIS, University of Bologna, Cesena, Italy; and Department of Cardiology (S.G.P.), University of Pavia, Italy.

This manuscript was sent to Michael Rosen, Consulting Editor, for review by expert referees, editorial decision, and final disposition.

Correspondence to Silvia G. Priori, MD, PhD, Director, Cardiovascular Genetics Program, Leon H. Charney Division of Cardiology, New York University School of Medicine, Smilow Research Building, Rm 701, 522 First Ave, New York, NY. E-mail silvia.priori@nyumc.org or silvia.priori@fsm.it

© 2010 American Heart Association, Inc.

Circulation Research is available at <http://circres.ahajournals.org>

DOI: 10.1161/CIRCRESAHA.110.218891

electrocardiographic pattern of coved type ST segment elevation in right precordial leads typical of Brugada syndrome.^{10,11} Shortly thereafter, it also became clear that sodium channel blockers do not invariably shorten the QT interval, suggesting that *SCN5A* mutations act through other mechanisms, questioning the “gain-of-function” paradigm that all LQT3 mutations lead to a common channel dysfunction.

This view is supported by the fact that “some” *SCN5A* mutations cause “overlapping syndromes” in which QT prolongation is associated with “loss-of-function” clinical phenotypes (Brugada syndrome or conduction defects).^{12,13–14}

We recently demonstrated that biophysical diversity of *SCN5A* mutations is a determinant of response to mexiletine in the clinical setting.¹⁵ Here, we bring the characterization of the diversity of *SCN5A* mutations to the next level by showing that the interplay between protein trafficking and biophysical abnormalities may detrimentally affect the response to sodium channel blockers and represent a hazard rather than a cure.

Methods

An expanded Methods section is available in the Online Data Supplement at <http://circres.ahajournals.org>.

Molecular Screening

Genetic analysis was performed by screening of the open reading frame of the *SCN5A*, *KCNH2*, *KCNQ1*, *KCNE1*, and *KCNE2* genes as we previously reported.¹⁶

Electrophysiology

Site-directed mutagenesis and transfection in HEK 293 cells were performed as we previously reported.¹⁵ Membrane currents were measured using whole-cell patch clamp procedures (details of procedures are provided in the Online Data Supplement).

Immunofluorescence and Immunoblotting for Quantification of Plasma Membrane Protein Expression

The distribution of Nav1.5 was accessed by polyclonal Nav1.5 in confocal microscopy. The total proteins and plasma membrane fractions were assessed by western blotting using standardized protocols. For a detailed description, see the Online Data Supplement.

Computer Simulation

Computer simulation was based on the Markovian model.¹⁷ For a detailed description see the Online Data Supplement.

Statistics

Data are presented as means \pm SE. Statistical comparisons were made using an unpaired 2-tailed *t* test or ANOVA with the Tukey post hoc test to evaluate the significance of differences between means. *P* < 0.05 was considered statistically significant.

Results

Clinical History of the Carrier of F1473S Mutation in the *SCN5A* Gene

The mutation we characterize here was identified in a patient born in 2003; no ECG was recorded at birth, and the baby was discharged as a healthy infant. At 12 months of age, he experienced 5 syncopal spells within a few days, was hospitalized and long-QT syndrome was diagnosed. Propranolol (4

Non-standard Abbreviations and Acronyms

APD	action potential duration
ER	endoplasmic reticulum
I_{sus}	sustained sodium current
LQT3	long-QT syndrome type 3
SSA	steady-state activation
SSI	steady-state inactivation
WT	wild type

mg/kg per day) was initiated, and a blood sample was sent to Maugeri Foundation for genetic screening. We sequenced the opening reading frame of *KCNQ1*, *KCNH2*, *SCN5A*, *KCNE1*, and *KCNE2* and identified a heterozygous single-nucleotide transition (4418T>C) in the *SCN5A* gene, leading to a single amino acid replacement at position 1473 (F1473S) (Figure 1A). This mutation was not present in either the parents of the index case or in 300 control DNA samples.

The patient remained asymptomatic for 2 years on β -blockers; however, in 2006, syncope recurred and torsade de pointes was documented; a ventricular-inhibited pacemaker was implanted, and the dose of β -blockers was increased. One year later, the patient experienced another syncopal episode, accompanied by several runs of torsade de pointes. Oral mexiletine was started in an attempt to shorten QT interval and to control arrhythmias; sinus rhythm was regained and QT duration appeared stable at day 1 of administration (Figure 1B, upper trace); unfortunately, the effect of mexiletine (60 mg tid) decayed as the treatment continued. After 10 days, QTc persistently exceeded 650 ms (Figure 1B, lower trace); furthermore, progressive worsening of intraventricular conduction with QRS widening, and occasional pacemaker capture failures (Figure 1C) were observed. At day 11, the patient developed incessant, intractable tachyarrhythmias and died. The clinicians who treated the patient contacted us and were confounded by the worsening clinical status during mexiletine treatment. The inspection of the available ECG showed QTc shortening just at the beginning of therapy followed by prolongation (Figure 1B). We attempted to understand this uncommon and paradoxical response to mexiletine by functional characterization of the mutant.

Functional In Vitro Characterization of F1473S

As shown in Figure 2A, F1473S depolarized the steady-state inactivation (SSI) curve by 18.9 mV and steady-state activation (SSA) curve by 4.4 mV. The SSI pattern of mutant channels was consistent with our previous data¹⁵ showing that mexiletine-insensitive mutations are those causing a depolarizing shift of SSI and it also produced a greater overlap of activation and inactivation relations. As a consequence, the window current was markedly enhanced. Recovery from inactivation is shown in Figure 2B.

Besides enlarged window current, F1473S showed a striking increase of I_{sus} . At -10 mV, F1473S channels continued

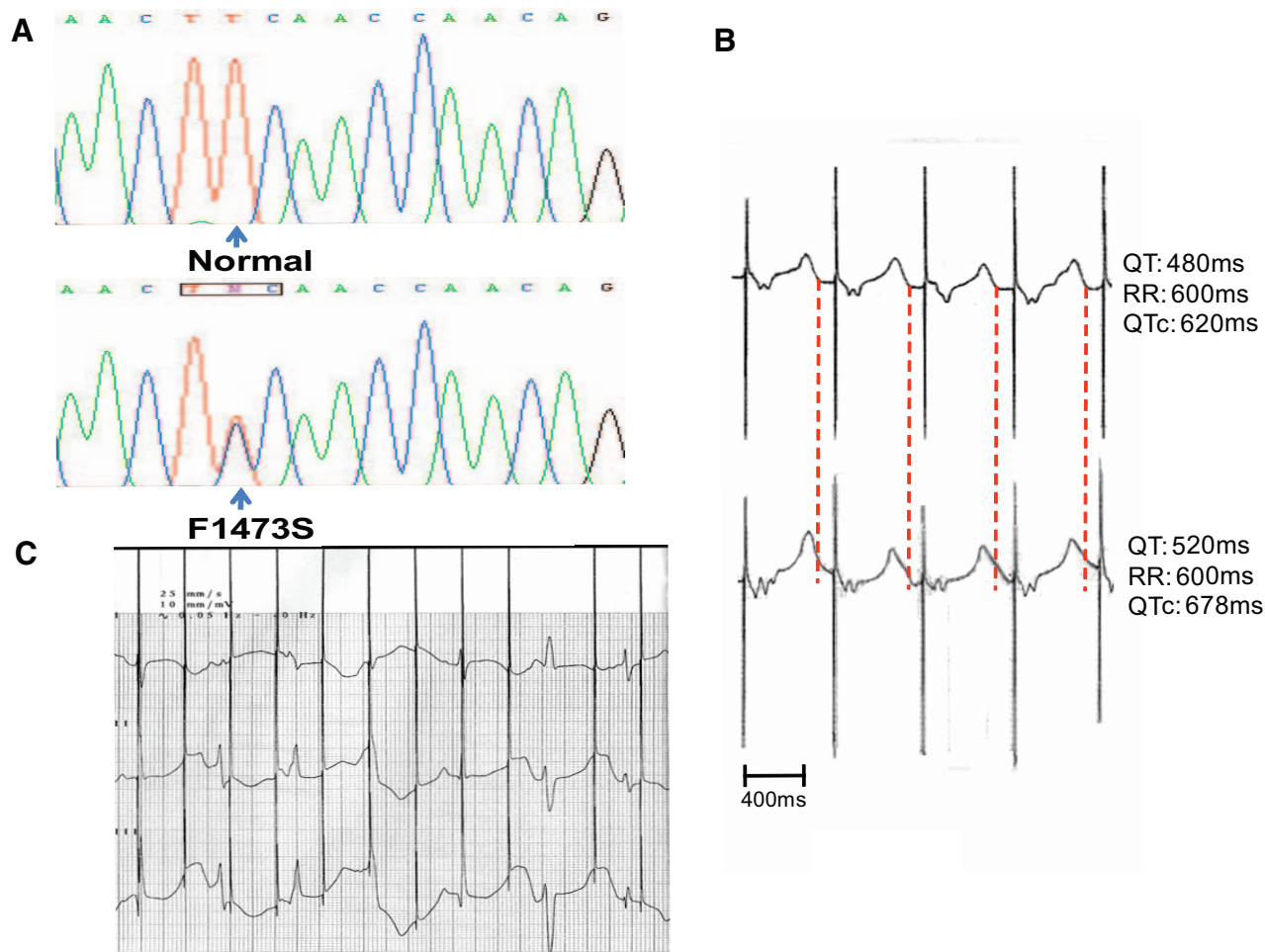


Figure 1. Mexiletine failed to shorten QTc and to prevent malignant ventricular arrhythmia. **A**, DNA sequence encoding a portion of DIII \approx DIV is shown for a normal control and for the index patient. The affected codon is enclosed by a rectangle. **B**, ECG recorded at day 1 (upper trace) and day 10 (lower trace) of mexiletine treatment. Further QTc prolongation is evident and the T wave is almost fused with the subsequent stimulation spike. **C**, ECG tracing recorded at day 10 on mexiletine showing failures of pacemaker capture with extremely prolonged cardiac repolarization.

to show 4.46 ± 0.74 pA/pF ($5.39 \pm 0.2\%$ of the peak current) at 150 ms as compared to 0.64 ± 0.22 pA/pF ($0.25 \pm 0.05\%$) in wild-type (WT) ($P < 0.0001$). Overall, F1473S showed a much higher I_{sus} than other mutations we previously characterized (Figure 2C).¹⁵

We further characterized the gain-of-function behavior by ramp voltage protocol (from -100 mV to $+50$ mV). F1473S conducted larger peak currents than WT (F1473S -6.38 ± 0.71 pA/pF, $n=9$ versus WT -2.28 ± 0.14 pA/pF, $n=8$; $P < 0.0001$), and the voltage of the peak was shifted by about $+20$ mV (F1473S -17.1 ± 3.5 mV, $n=9$ versus WT, -37.8 ± 3.1 mV, $n=8$; $P < 0.0001$). WT channels conduct current over a narrow range of voltages near -37 mV, whereas F1473S mutant channels conduct current over a broad range of voltages and increase the inward sodium current (Figure 2D).

We concluded that the remarkable increase of both the window current and the I_{sus} account for QT prolongation and the malignant clinical phenotype.

On the other hand, F1473S peak current density was unexpectedly reduced to 20% of WT (Figure 3A), suggesting a trafficking abnormality. This hypothesis was confirmed by

confocal microscopy experiments that showed an abnormal protein distribution characterized by clusters/aggregates retained in the cytoplasm (Figure 3B, F1473S). We attempted to colocalize such clusters to determine whether the mutant polypeptides were retained either in the endoplasmic reticulum (ER) (anti-calnexin antibody) or in the Golgi apparatus (anti-Golgin antibody). The F1473S-Nav1.5 clusters did not colocalize with Golgi (Figure 3C, f) and only mildly colocalized with ER (Figure 3C, c), suggesting that most of the abnormal protein is likely to be either free in the cytosol or segregated in yet unidentified subcellular domain(s).

Response of F1473S-Nav1.5 Channel to Exposure to Sodium Channel Blockers

We compared the tonic block of mexiletine in F1473S Nav1.5 with that observed in WT and in mexiletine-sensitive (R1626P) and mexiletine-insensitive mutations (S941N) that we previously characterized.¹⁵ Figure 4A shows that tonic block of peak current with $10 \mu\text{mol/L}$ mexiletine was significantly higher in R1626P compared with WT, S941N, and F1473S; no significant difference was found between F1473S and WT or the insensitive mutation, S941N. Consis-

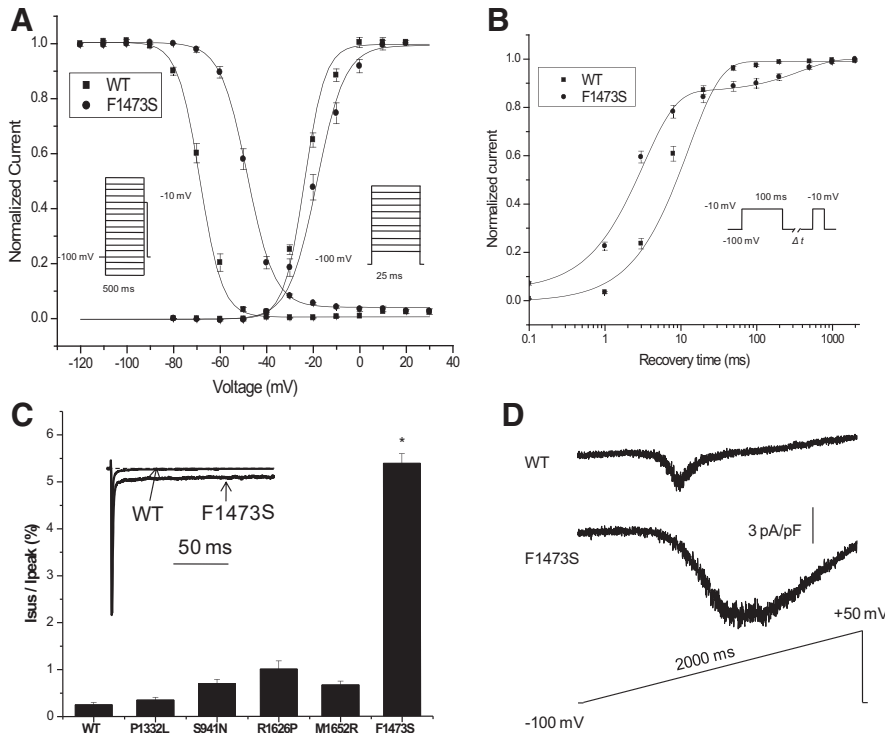


Figure 2. Gating properties of F1473S. **A**, The voltage dependence of SSI and SSA of F1473S, measured with standard pulse protocols shown in inset. Experimental data were fitted with Boltzmann relationships to obtain the parameters shown in the Table. **B**, Recovery from inactivation was assessed by the double-pulse protocol shown in inset and fitted using a biexponential function. Time constants and relative weights on averaged data are shown in Table. **C**, The amplitude of I_{sus} in F1473S expressed in percentage of peak current is more than 20-fold larger than in WT; and it is also significantly larger than in other severe LQT3 mutants, P1332L, S941N, R1626P, and M1652R. **D**, Original recording currents from WT and F1473S Nav1.5 in response to a ramp test.

tent with previous studies showing that sodium channel blockers inhibit preferentially I_{sus} versus peak current,¹⁸ tonic block of I_{sus} was proportionally stronger than tonic block of peak current with 10 μ mol/L mexiletine (Figure 4A). The tonic block of I_{sus} was similar among the 3 mutants.

An additional well-known mechanism underlying the LQT3 phenotype is the reopening of sodium channels over voltage ranges for which SSI and SSA overlap (ie, the window current). We tested the effect of 10 μ mol/L mexiletine on SSI and SSA in the F1473S mutation. SSI shifted toward the negative potential by -1.15 mV, SSA was slightly shifted toward the positive potential by 0.32 mV leaving the overlapping region substantially unchanged (Figure 4B).

Mexiletine Exposure and Trafficking

Previous studies suggested mexiletine rescued impaired trafficking observed in selected loss-of-function *SCN5A* mutants associated with Brugada syndrome.^{19–21} We therefore assessed whether the F1473S-Nav 1.5 trafficking defect could be rescued by the drug. F1473S channels incubated with mexiletine (10 μ mol/L for 48 hours) did not change their gating properties (data not shown) but showed significantly increased current density. Figure 4C shows that I_{Na} peak

current density at -5 mV increased by 42% after incubation but recorded in the absence of mexiletine, indicating that mexiletine does restore trafficking of F1473S. Interestingly, however, peak current density recorded in the presence of mexiletine (after incubation) was still increased by 32%, indicating that rescue effect overwhelmed the blocking effect.

Similar approach was used to quantify I_{sus} : (1) incubation with 10 μ mol/L mexiletine (48 hours) and recordings in the absence of mexiletine showed 46% increased I_{sus} density. The I_{sus} to peak current ratio remained the same as in untreated cells, implying that I_{sus} is increased by mexiletine incubation as a direct consequence of rescuing of the trafficking. (2) I_{sus} density recorded after incubation and in presence of 10 μ mol/L mexiletine remained same as control (untreated cells) indicating that mexiletine treatment did not decrease I_{sus} density because the rescue effect balanced out the block effect (Figure 4D).

Immunostaining with anti-hNav1.5 antibody confirmed that mexiletine incubation alleviates the trafficking impairment caused by F1473S. As shown in Figure 5A and 5B, after mexiletine incubation the F1473S-Nav 1.5 clusters were markedly reduced with a redistribution of the protein in the cytoplasm and in correspondence of the cell membrane (Figure 5B, f versus c). Analysis of the different cell fractions

Table. Biophysical Parameters of F1473S Mutant Channel

	Steady-State Inactivation			Steady-State Activation			Recovery From Inactivation		
	V1/2, mV	K, mV	n	V1/2, mV	K, mV	n	T1, ms (%)	T2, ms (%)	n
WT	-67.69 ± 0.87	5.37 ± 0.17	12	-23.08 ± 0.59	6.16 ± 0.20	9	8.29 (95.05)	170.38 (4.25)	9
F1473S	$-48.75 \pm 0.86^*$	5.14 ± 0.28	12	$-18.70 \pm 1.30^\dagger$	$7.27 \pm 0.22^\ddagger$	15	2.83 (81.80)	235 (14.88)	8

Because the functions for recovery from inactivation were fitted to the averaged data, error estimates on these parameters were not obtained. * $P < 0.001$, $^\dagger P < 0.05$, $^\ddagger P < 0.01$ compared with WT.

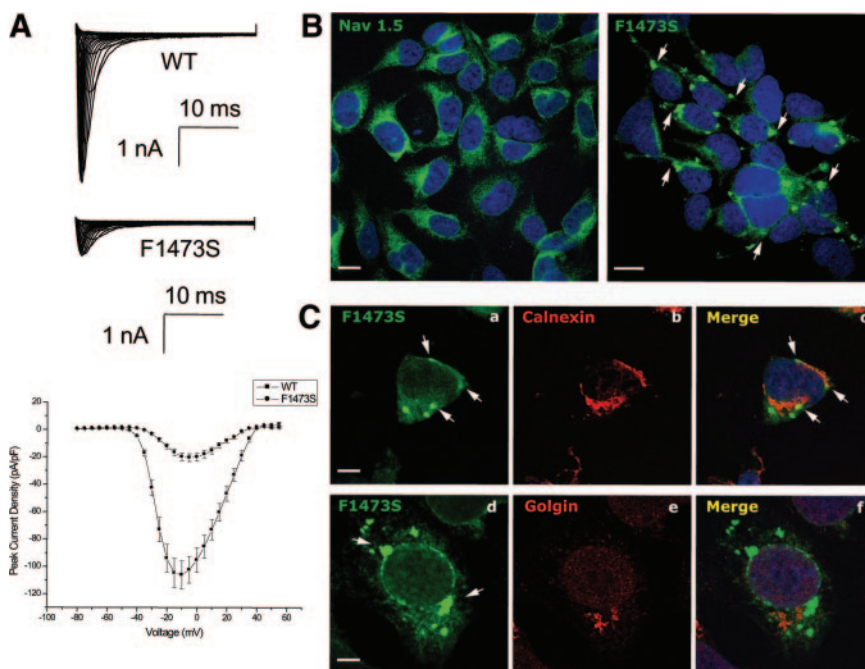


Figure 3. F1473S induced a reduced peak current in SCN5A channel. **A**, Representative whole-cell current traces in HEK293 cell expressing WT and F1473S channels. **Bottom**, Current-voltage relationship of peak inward current. F1473S reduced peak current by 80%. For example, at -10 mV, the peak current density is 106.24 ± 10.3 pA/pF, $n=10$ in WT and 20.00 ± 2.15 pA/pF, $n=33$ in F1473S; $P<0.0001$. **B**, Cells expressing either WT (left) or F1473S (right) SCN5A were immunostained with anti-SCN5A primary antibody (Alomone ASC-005) (green). The nuclei were highlighted by the DAPI staining (blue). **Scale bar**: 10 nm. WT channels were distributed mainly in the cytoplasm and on the plasma membrane; F1473S mutant channels show many condensed spots within the cytoplasm, suggesting a trafficking impairment (white arrows). **C**, Cytoplasmic distribution of F1473S mutant channel in HEK-SCN5A stable cell lines. Fixed cells were costained with the anti-SCN5A polyclonal antibody (a and d) (green) and either with anti-calnexin mAb for the ER (b) (red) or anti-Golgin 97 mAb for the Golgi Apparatus (e) (red). **Scale bar**:

10 nm. Protein localization was revealed by indirect immunofluorescence using DyLight 488-conjugated anti-rabbit IgG donkey antibodies. F1473S showed many condensed spots (white arrows) proximal to and partially colocalizing with the ER but not with the Golgi.

by Western blot showed that incubation with $10 \mu\text{mol/L}$ mexiletine increased the abundance of Nav-protein on the plasma membrane without affecting the total content of protein in whole cell homogenates (Figure 5C).

Overall, we conclude that exposure to $10 \mu\text{mol/L}$ mexiletine did not decrease I_{sus} , because the rescued trafficking of F1473S channel offset the blockade of I_{sus} . On the contrary, peak current (and the resulting window current) was significantly increased by mexiletine as the rescuing effect overwhelmed the blocking effect on peak current.

In Silico Evaluation of F1473S-Nav1.5 and Mexiletine Effects on Action Potential

We also investigated the consequences of the biophysical properties of F1473S-Nav1.5 on action potential by using a Markovian Na^+ channel model based from Clancy and Rudy²² (see the Online Data Supplement for details) tuned to simulate the mutant current behavior and incorporating it into a comprehensive action potential model of human ventricular myocyte. Figure 6 shows that the effects of F1473S on the voltage-dependence of activation, inactivation and increased window current (Figure 6A) and the time course of recovery from the inactivated state (Figure 6B) are correctly reproduced. Simulation of I_{sus} and response to a ramp test is shown in Online Figure II.

We then simulated the consequence of mexiletine exposure on action potential in heterozygote conditions by introducing into the model the reduction of peak I_{Na} , the reduction of the I_{sus} , the SSI shift and the rescuing effect according to the data obtained experimentally (see the Online Data Supplement for details). After mexiletine, APD prolonged (Figure 7A) and the time course of I_{Na} current during the plateau phase showed a significant reactivation of the window current that

prolonged the action potential. Interestingly at fast heart rates (eg, 120 bpm) adaptation of APD was impaired resulting in failure to capture (Figure 7B).

Discussion

Mutations associated with LQT3 are characterized by a gain-of-function,⁴ suggesting that the pharmacological reduction of I_{Na} could attenuate the QT prolongation. Because its inception this hypothesis seemed to gather rapid confirmation in experimental,⁷ as well as in clinical investigations^{8,9,23} and it supported the view that LQT3 patients would respond to such a “corrective” pharmacological treatment. Thus, the use of sodium channel blockers has been widely supported and it was incorporated into guidelines for clinical practice to reduce the arrhythmic burden with an appropriately cautious class IIb recommendation.²⁴

As more SCN5A mutations were studied over the years, it has become progressively clear that they may combine different electrophysiological properties and induce complex phenotypes.¹² Some mutations can bear, at the same time, gain-of-function and loss-of-function properties. We reported¹³ a single amino acid deletion (lysine at position 1500) resulting in long-QT syndrome, Brugada syndrome, and conduction disease in the same family. This observation was just one of several signals that raised concern that not all gain-of-function mutations should be considered equal and that the use of flecainide or mexiletine might be life saving for some but not for all LQT3 patients.¹¹

In 2007, we attempted to establish whether the clinical response to mexiletine could be predicted on the basis of the biophysical properties detected with heterologous expression of SCN5A mutants. Our data¹⁵ suggested that the single most important factor that correlates with a positive response to

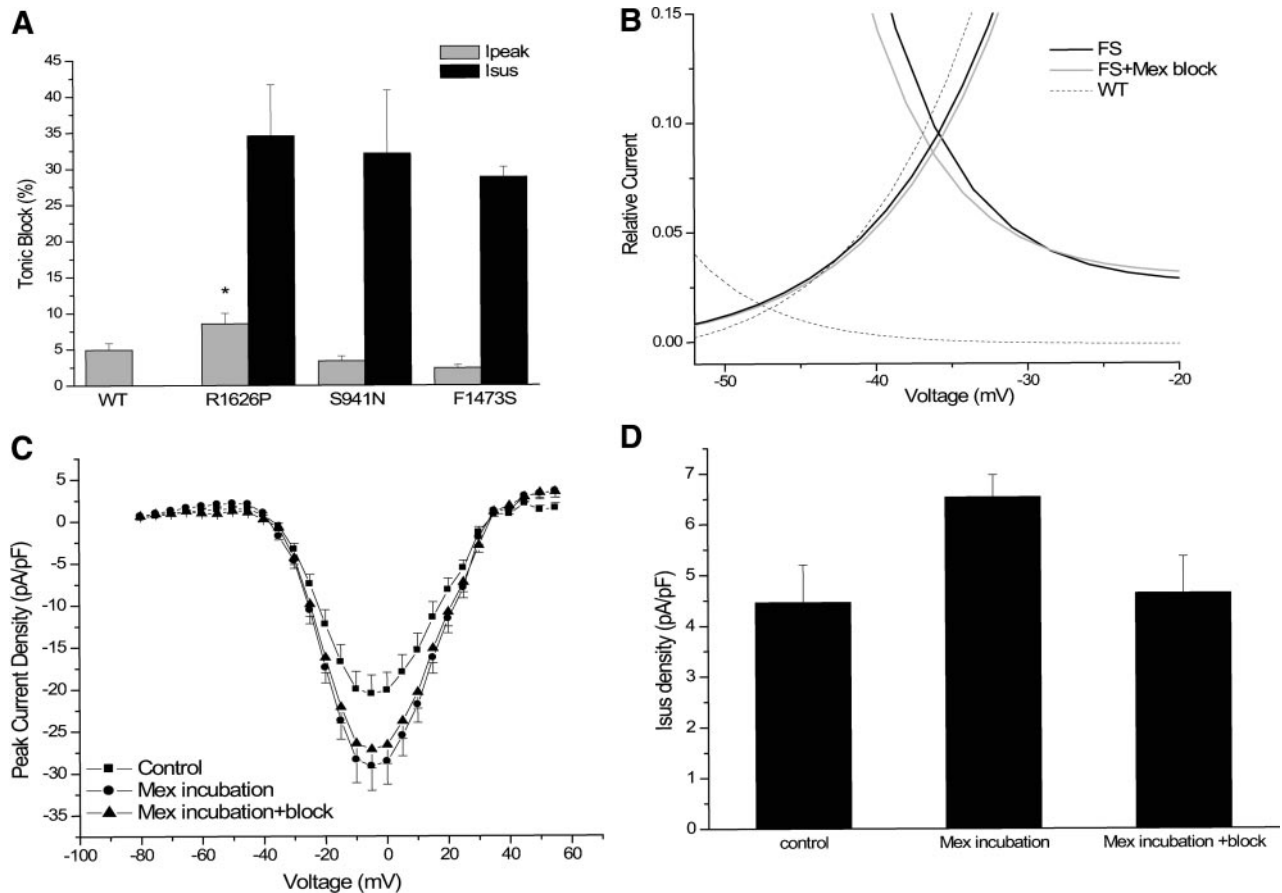


Figure 4. Rescue and block effect of mexiletine. **A**, Tonic block for WT, R1626P (mexiletine sensitive), S941N (mexiletine insensitive), and F1473S by 10 μ mol/L mexiletine (gray bars) was $4.9 \pm 0.9\%$, $8.5 \pm 1.5\%$, $3.4 \pm 0.6\%$, and $2.4 \pm 0.4\%$. * $P < 0.05$ compared with WT using 1-way ANOVA, followed by a Tukey post hoc test ($n = 5$ to 10 for each group). Fraction of I_{sus} blocked by 10 μ mol/L mexiletine (black bars) in WT, R1626P, S941N, and F1473S was $34.6 \pm 7.1\%$, $32.1 \pm 8.8\%$, and $28.8 \pm 1.4\%$ in R1626P, S941N, and F1473S, respectively ($n = 5$ to 10 for each group). Inhibition of I_{sus} was not significantly different among 3 mutations. **B**, F1473S depolarizing shift SSI produced an enlarged window current (black solid line) compared with WT (black dash line); effect of 10 μ mol/L mexiletine on window current was marked as gray solid line. **C**, Peak current density of 3 conditions: F1473S control (control, 20.54 ± 2.22 pA/pF at -5 mV, $n = 33$), F1473S incubated with 10 μ mol/L mexiletine for 48 hours with current recording in the absence of mexiletine (mex incubation, 29.17 ± 2.87 pA/pF at -5 mV, $n = 44$, $P < 0.05$ vs control), and F1473S incubated with 10 μ mol/L mexiletine for 48 hours and current recording in the presence of 10 μ mol/L mexiletine (mex incubation+block, 27.17 ± 2.3 pA/pF at -5 mV, $n = 36$, $P < 0.05$ vs control). **D**, I_{sus} density of 3 conditions: F1473S control (control, 4.46 ± 0.74 pA/pF, $n = 8$), F1473S incubated with 10 μ mol/L mexiletine for 48 hours with current recording in the absence of mexiletine (mex incubation, 6.53 ± 0.44 pA/pF, $n = 32$, $P < 0.05$ vs control), and F1473S incubated with 10 μ mol/L mexiletine for 48 hours and current recording in the presence of 10 μ mol/L mexiletine (mex incubation+block, 4.64 ± 0.72 pA/pF, $n = 16$, $P = NS$ vs control).

therapy is represented by a left-ward displacement of SSI. These findings highlighted the concept that knowing the in vitro consequences of mutants could guide clinical management.

The Heterogeneous Biophysical Properties of *SCN5A* Mutations in LQT3

Here, we characterize a novel mutant that seems to open another chapter, with therapeutic implications, in support of the view that the loss-of-function/gain-of-function paradigm may dangerously oversimplify our clinical approach to *SCN5A* mutation carriers²⁵ and that in vitro analysis of mutants might become a prerequisite to gene-specific therapy. Indeed, the evidence clearly indicates that in selected *SCN5A* mutations associated with a clinical phenotype suggestive of gain-of-function, the use of sodium channel blockers may result in harmful rather than curative effects.

The present investigation was prompted by a clinical case in which a patient affected by an early onset LQT3 showed no clinical improvement with mexiletine and possibly presented a worsening of the substrate leading to in-hospital death.

Interestingly, another mutation at the same site, F1473C, was recently reported to be insensitive to mexiletine,²⁶ and the carrier of the mutation continued to experience torsade de pointes after the drug, thus requiring implantable cardioverter defibrillator implantation and left stellate gangliectomy. The biophysical characterization of the F1473C reported by Bankston et al²⁷ is a completely different profile as compared with F1473S. F1473C causes a much smaller I_{sus} (0.6% versus 5.39% in F1473S) and it does not reduce the peak current density. These observations highlight the fact that it is not possible to predict functional properties based on the location of a mutation and that in-depth functional studies are required.

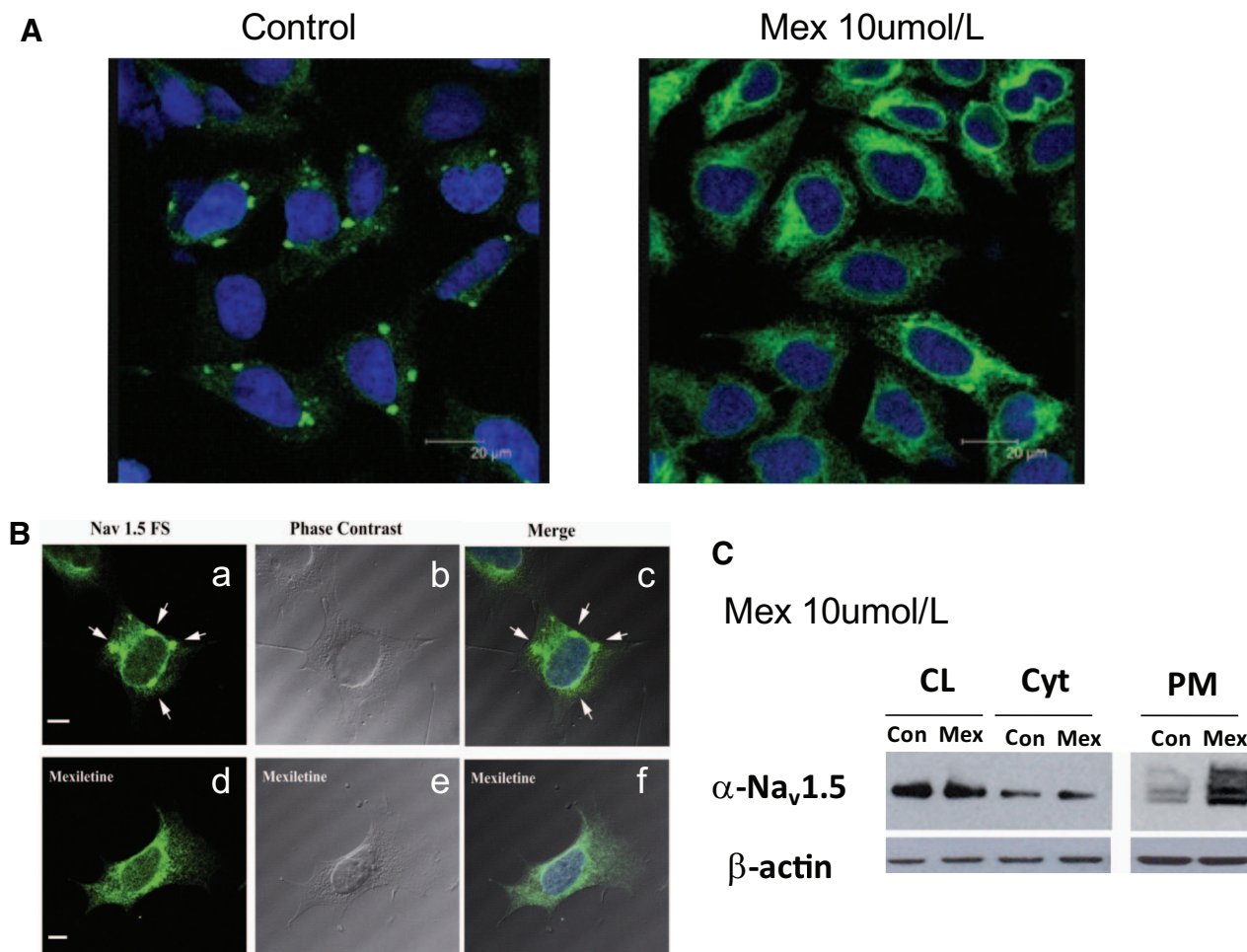


Figure 5. Rescued membrane expression of F1473S SCN5A channel with 10 μ mol/L mexiletine. **A**, Mexiletine incubation increased the cytoplasmic distribution of F1473S and released the intracellular condensed spots of F1473S. **Scale bar**: 20 nm. **B**, Confocal images of F1473S distribution with phase contrast in control condition (**top**) and with 10 μ mol/L mexiletine incubation (**bottom**). **Scale bar**: 10 nm. **C**, Plasma membrane fraction of F1473S SCN5A was increased by mexiletine incubation. PM indicates plasma membrane; Cyt, cytosol; CL, total cell lysate; Con, control, no mexiletine incubation; Mex, 10 μ mol/L mexiletine incubation for 48 hours. β -Actin was used as the normalizing control.

Increased I_{sus}^{28} and window current²⁹ are 2 known mechanisms for QT prolongation in LQT3. F1473S induces both to a considerable extent. Thus, 2 parallel biophysical abnormalities concur to generate the severe clinical phenotype observed in the proband. It is worth noting that whereas mexiletine has a strong blocking effect on I_{sus} it has only a mild blocking effect on peak current. In particular, we found

that a clinically relevant concentration of mexiletine (10 μ mol/L) blocked <3% of the peak current, whereas it blocked 28.8% of I_{sus} . As a result, the improved trafficking induced by mexiletine was offset for the I_{sus} but, because of the small peak I_{Na} blocking effect, the absolute amount of window current is greatly increased by this drug. When modeled in silico the effect of mexiletine resulted in a further

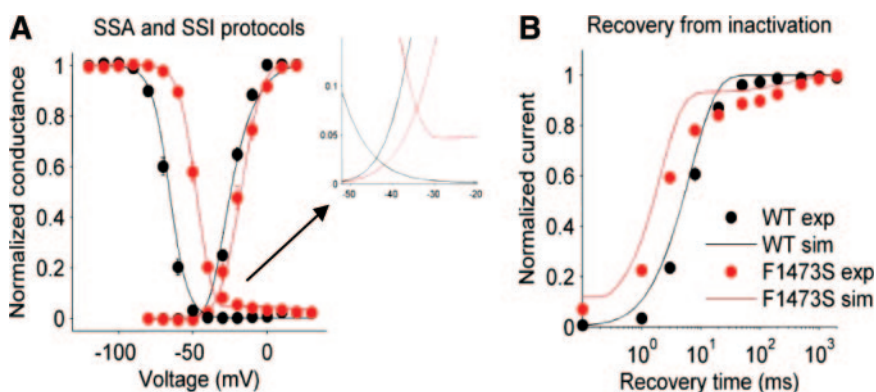


Figure 6. Experimentally determined and simulated effects of F1473S mutation on channel properties. **A**, SSI and SSA; the inset highlights in silico results in window current region. **B**, Results of recovery from inactivation. **Dots** represent data from in vitro experiments; **lines** represent simulated results.

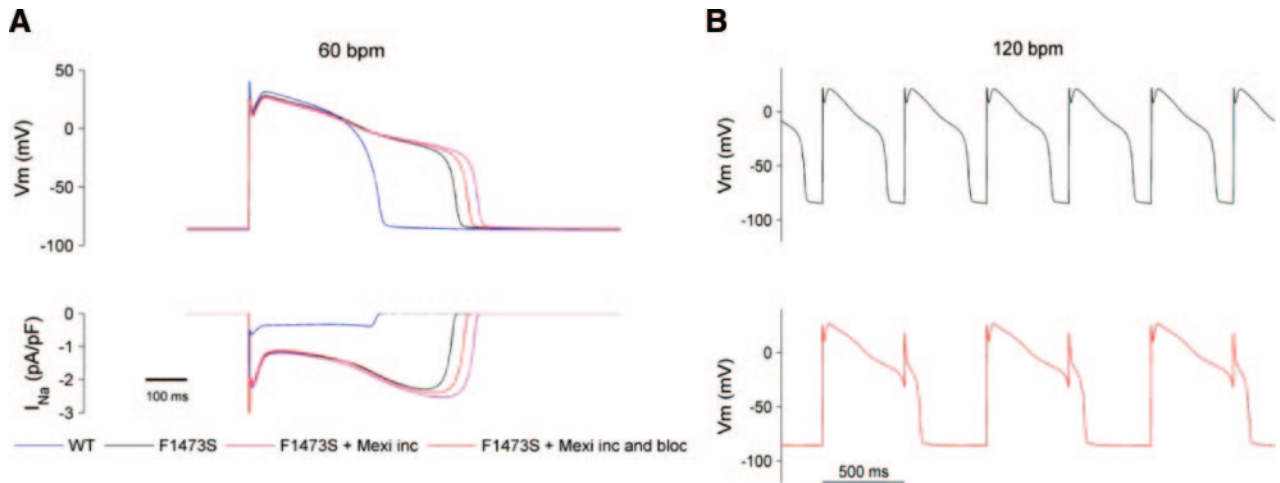


Figure 7. Simulation of the impact of the F1473S mutation and of mexiletine administration on the ventricular action potential. **A**, Effect of 10 $\mu\text{mol/L}$ mexiletine on sodium current (**bottom**) and ventricular cell APD (**top**) in presence of F1473S mutation at 60 bpm. Membrane potential and computed sodium currents for cells expressing WT (**blue line**) and heterozygous mutant (**black line**) channels. Incubation with mexiletine increases mutant channel expression and prolongs APD (**pink line**). Incorporation of block and rescue effect of mexiletine induces a smaller increase of sodium current and APD prolongation (**red line**). **B**, Treatment with 10 $\mu\text{mol/L}$ mexiletine (**red line**) further prolonged APD vs baseline (**black line**). At fast heart rates (120 bpm), the repolarization is not completed before the next heart beat thus inducing capture failures.

action potential prolongation, which is the likely culprit that tilted the balance toward the onset of life-threatening arrhythmias.

Mexiletine and the Unexplained Mechanisms for Rescuing Trafficking of Nav 1.5 Mutants

Mexiletine trafficking-rescuing activity has been demonstrated for several Nav1.5 mutants^{19–21,30} but the underlying mechanisms remain elusive. It has been suggested that drugs may act as “chemical chaperones” to promote protein folding and thereby facilitating the exit of mutant ion channel from the ER.^{31,32} In the case of F1473S, we observed only a small fraction of the mutant protein in the ER, thus suggesting that this mechanism is unlikely to play a major role in improving membrane localization. Ankyrin-G dependent SCN5A trafficking³³ is another potential mechanism. In collaboration with Mohler, we demonstrated that a human SCN5A mutation (E1053K) identified in a Brugada patient impairs ankyrin-G binding leading to a trafficking defect.³⁴ E1053 is localized in the predicted 9-aa ankyrin binding motif in the DII–III intracellular loop of Nav1.5 (VPIAVX[E]SD), but we cannot exclude that F1473S, which is in the DIII–DIV intracellular loop, similarly causes an impaired interaction with ankyrin-G.

Another poorly understood aspect of the efficacy of mexiletine in modulating protein localization is related to the concentration at which the effect is observed. Most of the studies used high concentrations of mexiletine, suggesting that a high dosage might be required to improve membrane targeting. Ackerman and colleagues were the first to report rescuing of G1743R³⁰ using clinical concentrations of mexiletine (10 $\mu\text{mol/L}$), pointing to the evidence that the efficacy is independent of the dosage; our data with 10 $\mu\text{mol/L}$ mexiletine support this view. Recently, it was suggested that only mutations located in extracellular loop region of the SCN5A could be rescued by sodium channel blockers³⁵; the

mutant studied here is located intracellularly; thus, it supports the idea that the position of the mutation is unlikely to be the key trafficking controlling factor of the Nav1.5 polypeptide.

The Need to Revisit Recommendations for the Use of Sodium Channel Blockers in LQT3

Improvement of trafficking in defective SCN5A mutations has been considered as a therapeutic strategy that should be applied irrespective of the biophysical profile of mutants; our study provides in vitro and in silico proof of concept that this assumption may be incorrect and potentially harmful. In an interesting editorial, Bezzina et al hypothesized that rescuing mutant channels with abnormal gating behavior could pose a proarrhythmic threat.³⁶ We now provide the first direct evidence of this hypothesis.

Our data establish a link between experimental data and clinical observations raising a warning flag to the “blanket indication” to use mexiletine in LQT3 patients. The improvement of trafficking of a gain-of-function mutant by mexiletine may be arrhythmogenic despite the channel blocking effect that would tend to counteract such a gain-of-function phenotype. The simulation shows that improvement of trafficking increases window current that is only minimally inhibited by mexiletine and thus contributes to APD prolongation.

It took the unfavorable outcome of the severely ill child affected by LQT3 to demonstrate that the loss-of-function/gain-of-function paradigm to classify SCN5A mutants is inadequate and that use of sodium channel blockers in LQT3 patients may be a double-edged sword posing a hazard to patient carriers of a SCN5A mutation with undefined electrophysiological properties.

Study Limitations

We acknowledge the presence of limitations in our study. In vitro experiments in heterologous systems are widely used but they do not get rid of factors that may importantly

modulate the effect of a mutation in the “real world,” such as temperature³⁷ or genetic background (influence of modulatory polymorphisms).^{20,38} Furthermore, in vitro experiments do not consider the important contribution to arrhythmogenesis of the signaling pathways, receptors, and autonomic modulation.

Sources of Funding

This work was supported by Telethon grants nos. GGP04066 and GGP06007 and by funds from the Ministero dell'Università e della Ricerca Scientifica e Tecnologica: FIRB RBNE01XMP4_006, RBLA035A4X_002, PRIN 2006055828_002, Italian Health Care Ricerca finalizzata RF-MAU-2007-641378.

Disclosures

None.

References

- Priori SG, Schwartz PJ, Napolitano C, Bloise R, Ronchetti E, Grillo M, Vicentini A, Spazzolini C, Nastoli J, Bottelli G, Folli R, Cappelletti D. Risk stratification in the long-QT syndrome. *N Engl J Med*. 2003;348:1866–1874.
- Priori SG, Napolitano C, Schwartz PJ, Grillo M, Bloise R, Ronchetti E, Moncalvo C, Tulipani C, Veia A, Bottelli G, Nastoli J. Association of long QT syndrome loci and cardiac events among patients treated with beta-blockers. *JAMA*. 2004;292:1341–1344.
- Clancy CE, Kass RS. Inherited and acquired vulnerability to ventricular arrhythmias: cardiac Na⁺ and K⁺ channels. *Physiol Rev*. 2005;85:33–47.
- George AL Jr. Inherited disorders of voltage-gated sodium channels. *J Clin Invest*. 2005;115:1990–1999.
- Wang Q, Shen J, Splawski I, Atkinson D, Li Z, Robinson JL, Moss AJ, Towbin JA, Keating MT. SCN5A mutations associated with an inherited cardiac arrhythmia, long QT syndrome. *Cell*. 1995;80:805–811.
- Ruan Y, Liu N, Priori SG. Sodium channel mutations and arrhythmias. *Nat Rev Cardiol*. 2009;6:337–348.
- Priori SG, Napolitano C, Cantu F, Brown AM, Schwartz PJ. Differential response to Na⁺ channel blockade, beta-adrenergic stimulation, and rapid pacing in a cellular model mimicking the SCN5A and HERG defects present in the long-QT syndrome. *Circ Res*. 1996;78:1009–1015.
- Schwartz PJ, Priori SG, Locati EH, Napolitano C, Cantu F, Towbin JA, Keating MT, Hammoude H, Brown AM, Chen LS. Long QT syndrome patients with mutations of the SCN5A and HERG genes have differential responses to Na⁺ channel blockade and to increases in heart rate. Implications for gene-specific therapy. *Circulation*. 1995;92:3381–3386.
- Windle JR, Geletka RC, Moss AJ, Zareba W, Atkins DL. Normalization of ventricular repolarization with flecainide in long QT syndrome patients with SCN5A:DeltaKQPQ mutation. *Ann Noninvasive Electrocardiol*. 2001;6:153–158.
- Priori SG, Napolitano C, Schwartz PJ, Bloise R, Crotti L, Ronchetti E. The elusive link between LQT3 and Brugada syndrome: the role of flecainide challenge. *Circulation*. 2000;102:945–947.
- Makita N, Behr E, Shimizu W, Horie M, Sunami A, Crotti L, Schulze-Bahr E, Fukuhara S, Mochizuki N, Makiyama T, Itoh H, Christiansen M, McKeown P, Miyamoto K, Kamakura S, Tsutsui H, Schwartz PJ, George AL Jr, Roden DM. The E1784K mutation in SCN5A is associated with mixed clinical phenotype of type 3 long QT syndrome. *J Clin Invest*. 2008;118:2219–2229.
- Bezzina C, Veldkamp MW, van Den Berg MP, Postma AV, Rook MB, Viersma JW, van Langen IM, Tan-Sindhunata G, Bink-Boelkens MT, van Der Hout AH, Mannens MM, Wilde AA. A single Na⁺ channel mutation causing both long-QT and Brugada syndromes. *Circ Res*. 1999;85:1206–1213.
- Grant AO, Carboni MP, Neplioeva V, Starmer CF, Memmi M, Napolitano C, Priori S. Long QT syndrome, Brugada syndrome, and conduction system disease are linked to a single sodium channel mutation. *J Clin Invest*. 2002;110:1201–1209.
- Antzelevitch C, Brugada P, Borggreffe M, Brugada J, Brugada R, Corrado D, Gussak I, LeMarec H, Nademanee K, Perez Riera AR, Shimizu W, Schulze-Bahr E, Tan H, Wilde A. Brugada syndrome: report of the second consensus conference: endorsed by the Heart Rhythm Society and the European Heart Rhythm Association. *Circulation*. 2005;111:659–670.
- Ruan Y, Liu N, Bloise R, Napolitano C, Priori SG. Gating properties of SCN5A mutations and the response to mexiletine in long-QT syndrome type 3 patients. *Circulation*. 2007;116:1137–1144.
- Napolitano C, Priori SG, Schwartz PJ, Bloise R, Ronchetti E, Nastoli J, Bottelli G, Cerrone M, Leonardi S. Genetic testing in the long QT syndrome: development and validation of an efficient approach to genotyping in clinical practice. *JAMA*. 2005;294:2975–2980.
- Clancy CE, Tateyama M, Kass RS. Insights into the molecular mechanisms of bradycardia-triggered arrhythmias in long QT-3 syndrome. *J Clin Invest*. 2002;110:1251–1262.
- Wang DW, Yazawa K, Makita N, George AL Jr, Bennett PB. Pharmacological targeting of long QT mutant sodium channels. *J Clin Invest*. 1997;99:1714–1720.
- Valdivia CR, Ackerman MJ, Tester DJ, Wada T, McCormack J, Ye B, Makielski JC. A novel SCN5A arrhythmia mutation, M1766L, with expression defect rescued by mexiletine. *Cardiovasc Res*. 2002;55:279–289.
- Tan BH, Valdivia CR, Song C, Makielski JC. Partial expression defect for the SCN5A missense mutation G1406R depends on splice variant background Q1077 and rescue by mexiletine. *Am J Physiol Heart Circ Physiol*. 2006;291:H1822–H1828.
- Pfahnl AE, Viswanathan PC, Weiss R, Shang LL, Sanyal S, Shusterman V, Kornblit C, London B, Dudley SC Jr. A sodium channel pore mutation causing Brugada syndrome. *Heart Rhythm*. 2007;4:46–53.
- Clancy CE, Rudy Y. Linking a genetic defect to its cellular phenotype in a cardiac arrhythmia. *Nature*. 1999;400:566–569.
- Benhorin J, Taub R, Goldmit M, Kerem B, Kass RS, Windman I, Medina A. Effects of flecainide in patients with new SCN5A mutation: mutation-specific therapy for long-QT syndrome? *Circulation*. 2000;101:1698–1706.
- Zipes DP, Camm AJ, Borggreffe M, Buxton AE, Chaitman B, Fromer M, Gregoratos G, Klein G, Moss AJ, Myerburg RJ, Priori SG, Quinones MA, Roden DM, Silka MJ, Tracy C, Smith SC Jr, Jacobs AK, Adams CD, Antman EM, Anderson JL, Hunt SA, Halperin JL, Nishimura R, Ornato JP, Page RL, Riegel B, Blanc JJ, Budaj A, Dean V, Deckers JW, Despres C, Dickstein K, Lekakis J, McGregor K, Metra M, Morais J, Osterspey A, Tamargo JL, Zamorano JL. ACC/AHA/ESC 2006 Guidelines for Management of Patients With Ventricular Arrhythmias and the Prevention of Sudden Cardiac Death: a report of the American College of Cardiology/American Heart Association Task Force and the European Society of Cardiology Committee for Practice Guidelines (writing committee to develop Guidelines for Management of Patients With Ventricular Arrhythmias and the Prevention of Sudden Cardiac Death): developed in collaboration with the European Heart Rhythm Association and the Heart Rhythm Society. *Circulation*. 2006;114:e385–e484.
- Priori SG. Inherited arrhythmogenic diseases: the complexity beyond monogenic disorders. *Circ Res*. 2004;94:140–145.
- Silver ES, Liberman L, Chung WK, Spotnitz HM, Chen JM, Ackerman MJ, Moir C, Hordof AJ, Pass RH. Long QT syndrome due to a novel mutation in SCN5A: treatment with ICD placement at 1 month and left cardiac sympathetic denervation at 3 months of age. *J Interv Card Electrophysiol*. 2009;26:41–45.
- Bankston JR, Yue M, Chung W, Spyres M, Pass RH, Silver E, Sampson KJ, Kass RS. A novel and lethal de novo LQT-3 mutation in a newborn with distinct molecular pharmacology and therapeutic response. *PLoS One*. 2007;2:e1258.
- Bennett PB, Yazawa K, Makita N, George AL Jr. Molecular mechanism for an inherited cardiac arrhythmia. *Nature*. 1995;376:683–685.
- Wang DW, Yazawa K, George AL Jr, Bennett PB. Characterization of human cardiac Na⁺ channel mutations in the congenital long QT syndrome. *Proc Natl Acad Sci U S A*. 1996;93:13200–13205.
- Valdivia CR, Tester DJ, Rok BA, Porter CB, Munger TM, Jahangir A, Makielski JC, Ackerman MJ. A trafficking defective, Brugada syndrome-causing SCN5A mutation rescued by drugs. *Cardiovasc Res*. 2004;62:53–62.
- Gong Q, Jones MA, Zhou Z. Mechanisms of pharmacological rescue of trafficking-defective hERG mutant channels in human long QT syndrome. *J Biol Chem*. 2006;281:4069–4074.
- Herfst LJ, Rook MB, Jongsma HJ. Trafficking and functional expression of cardiac Na⁺ channels. *J Mol Cell Cardiol*. 2004;36:185–193.
- Lowe JS, Palygin O, Bhasin N, Hund TJ, Boyden PA, Shibata E, Anderson ME, Mohler PJ. Voltage-gated Nav channel targeting in the heart requires an ankyrin-G dependent cellular pathway. *J Cell Biol*. 2008;180:173–186.

34. Mohler PJ, Rivolta I, Napolitano C, LeMaillet G, Lambert S, Priori SG, Bennett V. Nav1.5 E1053K mutation causing Brugada syndrome blocks binding to ankyrin-G and expression of Nav1.5 on the surface of cardiomyocytes. *Proc Natl Acad Sci U S A*. 2004;101:17533–17538.
35. Valdivia CR, Ruwaldt KM, Makielski JC. Trafficking defective SCN5A Brugada syndrome mutations rescue by different Class I antiarrhythmic drugs. *Heart Rhythm*. 2005;2:s136.
36. Bezzina CR, Tan HL. Pharmacological rescue of mutant ion channels. *Cardiovasc Res*. 2002;55:229–232.
37. Keller DI, Rougier JS, Kucera JP, Benammar N, Fressart V, Guicheney P, Madle A, Fromer M, Schlapfer J, Abriel H. Brugada syndrome and fever: genetic and molecular characterization of patients carrying SCN5A mutations. *Cardiovasc Res*. 2005;67:510–519.
38. Poelzing S, Forleo C, Samodell M, Dudash L, Sorrentino S, Anacletio M, Troccoli R, Iacoviello M, Romito R, Guida P, Chahine M, Pitzalis M, Deschenes I. SCN5A polymorphism restores trafficking of a Brugada syndrome mutation on a separate gene. *Circulation*. 2006;114:368–376.

Novelty and Significance

What Is Known?

- Long QT syndrome type 3 (LQT3) is caused by *SCN5A* mutations characterized by “gain-of-function” of the Nav 1.5 channel.
- In clinical practice, sodium channel blockers are used to reduce sodium current and are considered a gene-specific therapy for LQT3.
- *SCN5A* mutations characterized by “loss-of-function” are often caused by trafficking defect and can be rescued by sodium channel blockers.

What New Information Does This Article Contribute?

- Sodium channel blockers can prolong QT interval and worsen arrhythmias in carriers of selected *SCN5A* mutations.
- Bench study may be used to personalize therapy for LQT3 patients.

SCN5A mutations that increase the function of the sodium channel cause LQT3, whereas mutations that reduce the

function of the channel cause the Brugada syndrome. Based on the assumption that in all LQT3 patients, there is an increase in sodium current, sodium channel blockers have been proposed as an effective therapy for LQT3. In this study, we demonstrate that the F1473S mutation not only increases sustained current and window current but also causes a trafficking defect of the sodium channel, thus combining gain-of-function and loss-of-function changes. The effect of mexiletine on F1473S channels is deleterious, because even though the drug reduces the late component of sodium current, it also increases the number of channels on membrane. The net result is an increase in sodium current. Our findings suggest that the use of sodium channel blockers may be hazardous to some LQT3 patients and suggest that functional characterization of mutants may guide mutation-specific treatment of the disease.

Trafficking Defects and Gating Abnormalities of a Novel *SCN5A* Mutation Question Gene-Specific Therapy in Long QT Syndrome Type 3

Yanfei Ruan, Marco Denegri, Nian Liu, Tiziana Bachetti, Morena Seregni, Stefano Morotti, Stefano Severi, Carlo Napolitano and Silvia G. Priori

Circ Res. 2010;106:1374-1383; originally published online March 25, 2010;
doi: 10.1161/CIRCRESAHA.110.218891

Circulation Research is published by the American Heart Association, 7272 Greenville Avenue, Dallas, TX 75231
Copyright © 2010 American Heart Association, Inc. All rights reserved.
Print ISSN: 0009-7330. Online ISSN: 1524-4571

The online version of this article, along with updated information and services, is located on the
World Wide Web at:

<http://circres.ahajournals.org/content/106/8/1374>

Data Supplement (unedited) at:

<http://circres.ahajournals.org/content/suppl/2010/03/25/CIRCRESAHA.110.218891.DC1>

Permissions: Requests for permissions to reproduce figures, tables, or portions of articles originally published in *Circulation Research* can be obtained via RightsLink, a service of the Copyright Clearance Center, not the Editorial Office. Once the online version of the published article for which permission is being requested is located, click Request Permissions in the middle column of the Web page under Services. Further information about this process is available in the [Permissions and Rights Question and Answer](#) document.

Reprints: Information about reprints can be found online at:
<http://www.lww.com/reprints>

Subscriptions: Information about subscribing to *Circulation Research* is online at:
<http://circres.ahajournals.org/subscriptions/>

Supplement Material

Molecular Screening

Genetic analysis was performed by screening of the open reading frame of the *SCN5A*, *KCNH2*, *KCNQ1*, *KCNE1* and *KCNE2* genes as we previously reported ¹.

Site-directed Mutagenesis and Transfection in HEK 293 Cells

The *SCN5A* mutations were engineered into wild-type (WT) cDNA cloned in pcDNA3.1 (Invitrogen, Carlsbad, Calif) and confirmed by sequence analysis of the entire cDNA of *SCN5A*. HEK 293 cells were transfected with equal amount of Na⁺ channel α and β_1 subunit by lipofectamine as we previously described ².

Electrophysiology

Membrane currents were measured using whole-cell patch clamp procedures, with Axopatch 200B amplifiers (Axon Instruments, Foster City, CA). Internal pipette solution contained (mmol/L) aspartic acid 50, CsCl 60, Na₂-ATP 5, EGTA 11, HEPES 10, CaCl₂ 1, and MgCl₂ 1, with pH 7.4 adjusted with CsOH. External solutions consisted of (mmol/L) NaCl 130, CaCl₂ 2, CsCl 5, MgCl₂ 1.2, HEPES 10, and glucose 5, with pH 7.4 adjusted with CsOH. In experiments designed to measure the voltage dependence of activation, external Na⁺ was reduced to 30 mmol/L with N-methyl-glucamine used as a Na⁺ substitute. Recordings were made at room temperature. Holding potentials were -100 mV. Sustained sodium current (*I*_{sus}) was measured 150 ms after depolarization to -10 mV and determined by subtracting background currents measured in the presence of tetrodotoxin (30 μ mol/L, Sigma) from tetrodotoxin-free records. This subtraction procedure was also used for voltage ramp experiments. Steady-state inactivation was determined after application of conditioning pulses (500 ms) applied to a series of

voltages with an interpulse interval of 5 seconds for control and 30 seconds for mexiletine. Steady-state activation was estimated by measuring peak sodium current during a variable test potential. Current at each membrane potential was divided by the electrochemical driving force for sodium ions and normalized to the maximum sodium conductance. Data for the voltage dependence of activation and inactivation were fitted with the Boltzmann equation. Recovery from inactivation was measured in paired pulse experiments. Details of pulse protocol are given schematically in the figure. Data for the time course of recovery were fitted with functions of 2 exponentials. Tonic block (TB) was measured at 0.033 Hz after steady state was achieved in the presence of mexiletine. In drug rescue experiments, freshly prepared 10 μ mol/L mexiletine was added to the culture media.

Immunofluorescence

For immunofluorescence (IF) experiments HEK293 cells were seeded on 0.1% gelatin-coated coverslips and allowed to attach for 24 h, where indicated 10 μ mol/L mexiletine was added for 48 hours. Following PBS washed cells were fixed with 4% PFA for 10 min and permeabilised with 0.2% Triton for 10 min. Blocking of unspecific sites were achieved by incubation with 10% BSA for 1 hour at room temperature. Primary antibodies used were: polyclonal Nav1.5 (Alomone, ASC-005, 1:100), monoclonal Calnexin (Alexis, clone AF18, 1:200), monoclonal Golgin 97 (Molecular Probes, CDF4, 1:50). Secondary antibodies used were: DyLight 488-conjugated donkey anti-rabbit IgG and Dy-Light-conjugated 594-conjugated donkey anti-mouse IgG (Jackson Laboratories, 1:100). The coverslips were then mounted using a DAPI-containing mounting medium (Vectashield, Vector Laboratories, Burlingame, CA).

Confocal microscopy was performed with a Leica TCS-SP2 digital scanning confocal microscope equipped with a HCX PL APO 40x/numerical aperture =1.25 oil immersion objective. We used the 488-nm Argon laser line for excitation of DyLight 488-conjugated donkey anti-rabbit IgG (detected at 500-530 nm) and the 594 nm He/Ne laser line for excitation of Dy-Light-conjugated 594-conjugated donkey anti-mouse IgG (detected at 580-630 nm). The pinhole diameter was kept at Airy 1. Images were exported to Adobe Photoshop (Adobe Systems, Mountain View, CA).

Immunoblotting for Quantification of Plasma Membrane Protein Expression

First we confirmed that the I_{Na} current observed in stable cell lines expressing F1473S-Nav 1.5 was identical to the current observed in cells with transient expression of the mutant α and β_1 subunit and we were able to show that the same large I_{sus} , reduced peak current, trafficking defect and gating properties were also present in the transiently transfected cells expressing F1473S-Nav1.5 (Data not shown). HEK 293 cells which stably expressed F1473S SCN5A were lysed and total proteins extracted; plasma membrane and cytosolic fractions were isolated using a plasma membrane protein extraction kit according to manufacturer's instructions (Biovision).

Total proteins (15 micrograms/sample, quantified by the BCA assay) were resolved by SDS-gel electrophoresis on Novex 4–12% BisTris gradient gels using MES-SDS buffer (Invitrogen), and blotted on nitrocellulose membranes using a submarine system (Invitrogen). A monoclonal anti-human Nav1.5 antibody (1:500, Alomone, Asc-005) was used to probe for the sodium channel while a polyclonal anti β -actin antibody (1:5000, Affinity Bioreagents) was used to detect a reference protein. Secondary antibodies were conjugated with HRP (1:3000, Promega). Mouse heart was used as positive control.

Specific signals were developed using the Supersignal West Pico Chemiluminescent substrate (Pierce) and detected using X-ray films (Kodak).

Computer Simulation

Na⁺ Current Model Simulation

The Markovian Na⁺ channel model was based on the structure proposed by Clancy and Rudy ³ (Online Figure I). The whole-cell I_{Na} current is given by:

$$I_{Na} = G_{Na} * P_o * (V - E_{Na})$$

where the variable P_O represents the sum of the probabilities to be in the open states (O and LO), V is the membrane potential, E_{Na} is the Na⁺ Nerst potential and G_{Na} is the maximum conductance. The expressions of the transition rates are reported in Online Table I.

The transition rate parameters were identified by a fitting procedure to simulate the experimental data of whole-cell cardiac I_{Na} from HEK cells expressing WT or F1473S SCN5A. The following voltage-clamp protocols were simulated for parameter identification: steady-state activation and inactivation, recovery from inactivation, voltage ramp and long-depolarization voltage step to assess sustained I_{Na}. The model results for each protocol were compared with experimental data. The transition rates that maximally influence each voltage-clamp protocol were mainly identified in a previous study⁴. Namely, a₂ and a₄ were modified to reproduce the experimental data on steady-state activation; a₅ was tuned to correctly simulate the channel availability curve; a₆, b₆ and a₇, b₇ were adjusted to represent the observed characteristics of recovery from inactivation, a₅, b₆, b₇ were modified to reproduce the response to voltage ramp in the mutant channels and the ratio a₈/b₈ was tuned to reproduce the experimental data

accounting for sustained I_{Na} . The values proposed by Grandi et al.⁴ were chosen where possible as initial guesses in the identification procedure of the transition rate parameters that allowed the best fitting of our WT data. The identified WT set was subsequently used as initial guess to identify the F1473S channel parameters. Two parameters of the F1473S set were tuned to reproduce the effect of mexiletine treatment: P_{2a5} was modified to introduce the SSI shift and P_{1a8} to reduce sustained sodium current (Online Table II). Matlab 7 and Simulink (The MathWorks Inc.- Natick, Mass) were used for all the numerical computations.

Action Potential Simulation

The ventricular AP was simulated using the Ten Tusscher-Panfilov model of human epicardial ventricular myocyte⁵ as modified by Severi et al. to correctly reproduce the experimental APD inverse dependence on extracellular calcium concentration⁶. Extracellular calcium concentration was set to the physiological value of 1.15 mmol/L. Since mutant patients reveal stronger sustained sodium current and thereby higher intracellular sodium concentration, the initial value of this concentration was set at 15 mmol/L in order to reach the steady-state condition quickly. The original formulation of the I_{Na} current was replaced with the above Markov model. To analyze the effects of mutations on cardiac action potential in the heterozygous condition of F1473S patients, we replicated conditions with different percentage of mutant and WT sodium channels. Maximal conductance G_{Na} at 37°C was set to 57.5 mS/ μ F for WT and it was reduced to 20% (11.5 mS/ μ F) in F1473S to take into account the trafficking defect of mutant channels. The kinetic rates were normalized to 37°C a Q10 of 2.1⁷. Pacing was simulated by a current pulse train (pulse duration: 1 ms) of 52 A/F in amplitude with

different frequencies (from 30 to 120 bpm, i.e. from 0.5 to 2 Hz). A variable order solver based on the numerical differentiation formulas (NDFs) was used to numerically solve the model equations (ode15s) ⁸. The stimulation was maintained at least for 200 sec. We assumed that before treatment with mexiletine in an heterozygote carrier of the F1473S mutation 50% WT proteins are entirely on the cell membrane whereas only 20% of the 50% defective trafficking F1473S-Nav1.5 are available. After exposure to mexiletine we assumed that the 50% of WT current is blocked by 5% (see experimental data in Fig. 4A) and that the F1473S current is increased by 32% by concurrent blocking and rescuing effect of mexiletine.

Statistics

Pclamp9.2 (Axon Instruments, Foster City, CA) and Excel (Microsoft, Seattle, WA) were used for data acquisition and analysis. Data are presented as mean values \pm S.E. Statistical comparisons were made using an unpaired 2-tailed t test or ANOVA with the Tukey post hoc test to evaluate the significance of differences between means. $P < 0.05$ was considered statistically significant.

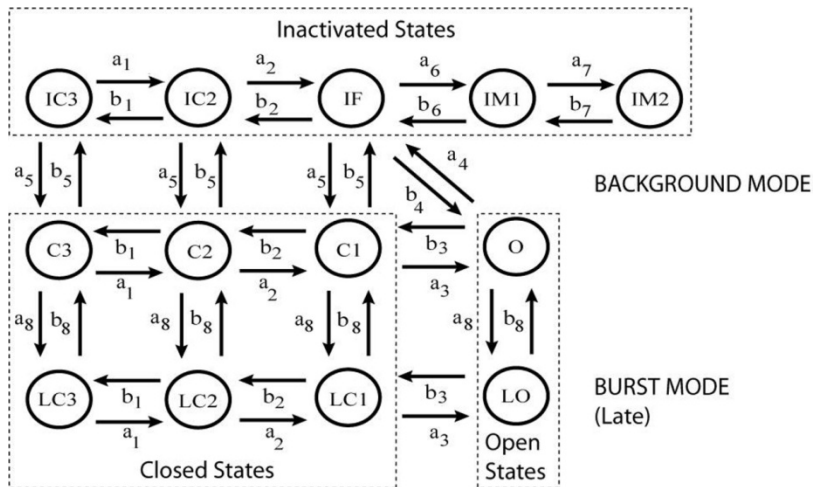
Online Table I - Transition rate expressions (ms^{-1}).

Transition rates
$a_1 = P_{1a1} / (1 + \exp((-V_m + P_{2a1})/P_{3a1}))$
$a_2 = P_{1a1} / (1 + \exp((-V_m + P_{2a2})/P_{3a2}))$
$a_3 = P_{1a3} / (1 + \exp((-V_m + P_{2a3})/P_{3a1}))$
$b_1 = P_{1b1} \exp((-V_m + P_{2a1})/P_{2b1})$
$b_2 = P_{1b2} \exp((-V_m + P_{2b2})/P_{2b1})$
$b_3 = P_{1b3} \exp((-V_m + P_{2b3})/P_{2b1})$
$a_4 = P_{1a4} \exp((V_m - P_{2a1})/P_{2a4})$
$a_5 = (P_{1a5} / (1 + \exp((V_m + P_{2a5})/P_{3a5}))) (P_{7a5} + P_{4a5} / (1 + \exp((-V_m + P_{5a5})/P_{6a5})))$
$a_6 = a_4 / P_{1a6}$
$b_4 = (a_3 a_4 a_5) / (b_3 b_5)$
$b_5 = P_{1b5} + P_{2b5} (V_m - P_{2a1})$
$b_6 = P_{1b6} \exp((-V_m + P_{2a1})/P_{2b6}) + P_{5b6} / (1 + \exp((-V_m + P_{4b6})/P_{3b6})))$
$a_7 = P_{1a7} \exp((V_m - P_{2a1})/P_{2a7})$
$b_7 = P_{1b7} \exp((-V_m + P_{2a1})/P_{2b7}) + P_{5b7} / (1 + \exp((-V_m + P_{4b7})/P_{3b7})))$
$a_8 = P_{1a8}$
$b_8 = P_{1b8}$

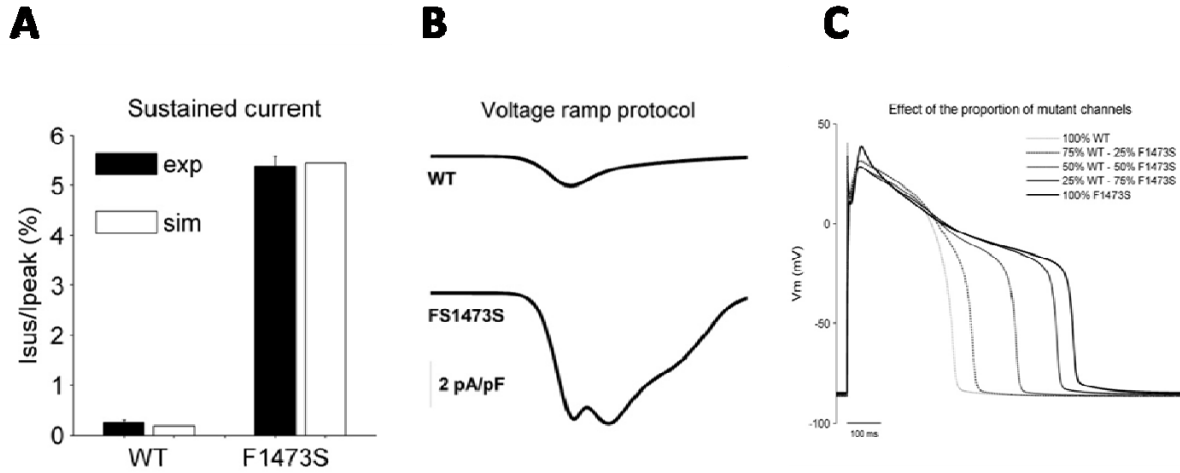
Online Table II – Na⁺ channel model parameters for WT and F1473S channels (with and without mexiletine treatment).

Parameters	WT	F1473S	
		+ mexi	
P _{1a1}	62.5	25	
P _{2a1}		5.4e ⁻³	
P _{3a1}	15	30	
P _{2a2}	-5.4e ⁻³	-6.0054	
P _{3a2}	17	7	
P _{1a3}	500	27	
P _{2a3}	29.9946	-5.4e ⁻³	
P _{1b1}	0.47925	0.1917	
P _{2b1}		20.3	
P _{1b2}	0.5	0.2	
P _{2b2}		4.9946	
P _{1b3}	0.55	0.22	
P _{2b3}		9.9946	
P _{1a4}	1.175	5.1	
P _{2a4}	90	45	
P _{1a5}	0.021	0.265	
P _{2a5}	71.9946	56.9946	57.9946
P _{3a5}		6	
P _{4a5}	0	400	
P _{5a5}		29.9946	
P _{6a5}		7	
P _{7a5}		1	
P _{1b5}	0.126	0.42	
P _{2b5}		2e ⁻⁶	
P _{1a6}	50	17	
P _{1b6}		3e ⁻⁴	
P _{2b6}	11.3944	13	
P _{5b6}	0	0.25	
P _{3b6}		5	
P _{4b6}		-18.0054	
P _{1a7}	3.543e ⁻³	3.19e ⁻³	
P _{2a7}		23.27	

P _{1b7}	8	5.8362979979338	
		8 e ⁻⁵	
P _{2b7}	35.9898	27	
P _{3b7}		3	
P _{4b7}		-30.0054	
P _{5b7}	0	4.5e ⁻³	
P _{1a8}	1.4e ⁻⁶	4.9e ⁻⁶	1.5e ⁻⁶
P _{1b8}		9.5e ⁻⁴	



Online Figure I. Markov model of the cardiac Na⁺ channel. The channel model contains background (upper nine states) and burst (lower four states) gating modes. The burst mode reflects a population of channels that transiently fail to inactivate.



Online Figure II. (A) Experimentally determined and simulated sustained sodium current for WT and F1473S channels. (B) Simulation of WT and F1473S current in response to the ramp test shown in Figure 2D. (C) Effect of F1473S on action potential duration (APD). The APD prolongation is related to the proportion of mutant channel.

References

1. Napolitano C, Priori SG, Schwartz PJ, Bloise R, Ronchetti E, Nastoli J, Bottelli G, Cerrone M, Leonardi S. Genetic testing in the long QT syndrome: development and validation of an efficient approach to genotyping in clinical practice. *Jama*. 2005;294:2975-2980.
2. Ruan Y, Liu N, Bloise R, Napolitano C, Priori SG. Gating properties of SCN5A mutations and the response to mexiletine in long-QT syndrome type 3 patients. *Circulation*. 2007;116:1137-1144.
3. Clancy CE, Tateyama M, Kass RS. Insights into the molecular mechanisms of bradycardia-triggered arrhythmias in long QT-3 syndrome. *J Clin Invest*. 2002;110:1251-1262.
4. Grandi E, Puglisi JL, Wagner S, Maier LS, Severi S, Bers DM. Simulation of Ca-calmodulin-dependent protein kinase II on rabbit ventricular myocyte ion currents and action potentials. *Biophysical journal*. 2007;93:3835-3847.
5. ten Tusscher KH, Panfilov AV. Alternans and spiral breakup in a human ventricular tissue model. *Am J Physiol Heart Circ Physiol*. 2006;291:H1088-1100.
6. Severi S, Corsi C, Cerbai E. From in vivo plasma composition to in vitro cardiac electrophysiology and in silico virtual heart: the extracellular calcium enigma. *Philosophical transactions*. 2009;367:2203-2223.
7. Maltsev VA, Undrovinas AI. A multi-modal composition of the late Na⁺ current in human ventricular cardiomyocytes. *Cardiovascular Research*. 2006;69:116-127.
8. Shampine LF, Reichelt MW. The MATLAB ODE Suite. *SIAM Journal on Scientific Computing*. 1997;18:1-22.